

NUMERICAL STUDY ON ELASTO-PLASTIC BEHAVIOR OF PIPE-SECTIONED PIER-PILE INTEGRAL STEEL STRUCTURE

Takayuki Omori¹, Akira Kasai², and Rei Kohara²

¹ Oriental Consultants Co., Ltd
3-12-1 Honmachi Shibuya-ku, -Tokyo, Japan
e-mail: ohmori@oriconsul.com

² Kumamoto University Graduate School of Science and Technology
2-39-1 Chuoku Kurokami, Kumamoto City, Japan
kasai@kumamoto-u.ac.jp, 164d8817@st.kumamoto-u.ac.jp

Keywords: Pier-Pile Integral Steel Structures, Compression Strength, Effective Buckling Length, Pipe Section, Residual Stress

Abstract. *Pier-Pile integral structures provide construction works with many environmental and landscape advantages. For example, the space required to construct these structures is smaller than that of other bridges due to the footing being removed, meaning that it is not necessary to greatly change the surroundings of these bridges. While there are environmental and landscape advantages, there are also a few demerits for the overall landscape designs, including demerits in the design of this proposed structure which consists of relatively slender parts. This proposed structure has already been constructed in areas where possibility of a severe earthquake is low. However, some problems that have yet to be examined are related to the use of this proposed structure in areas where earthquakes are frequent. Lacking detailed studies of its behavior during severe earthquakes, it is currently difficult to construct these structures in Japan. Consequently, it is necessary to investigate in detail limited performance about compression and bending moment, and earthquake-resistant performance of these structures in order to resolve these problems.*

The authors had previously clarified the relationship between the rigidity of the ground and the effective buckling length, and the compressive strength of the Pier-Pile Integral Steel Structure. Moreover, we had proposed a simplified formula using a proposed characteristic value, and had revealed the relationship between effective buckling length and compressive strength of the Pier-Pile Integral Steel Structure.

In this paper, we verify the compressive strength after confirming the residual stress of the ERW (Electric Resistance Welded) pipes. Moreover, the relationship with the Euler curve and the load-bearing capacity curve of box-shaped cross-section from the Japanese standards is clarified.

1 INTRODUCTION

Pier-Pile integral structures provide construction works with many environmental and landscape advantages. For example, the space required to construct these structures is smaller because there are no footings, which avoids changing topography and protects the landscape. Some examples of the use of Pier-Pile integral structures include the temporary gantry in Japan and the pedestrian bridge [1] in other parts of the world. (*Figure 1: Example of Pier-pile integral structure.*) However, construction of these structures presents a few problems. In particular, damaged areas cannot be identified after being subjected to a major earthquake. Therefore, it is currently difficult to construct these structures in Japan, a country where major earthquakes frequently occur. It is necessary to understand compression and bending behavior of these members, earthquake-resistant performance, and limit performance in detail in order to tackle these problems.



Figure 1: Example of Pier-pile integral structure.

In accordance with the Japanese standards [2; herein after Japan Standard II], piers are designed based on the capacity stress obtained from the load-bearing capacity curve after designing the slenderness ratio parameter $\bar{\lambda}$ from the effective length derived from boundary condition. However, in the case of Pier-Pile integral structures, it is hard to decide the effective buckling length for calculating slenderness ratio parameter $\bar{\lambda}$ as the lower part of the pier is supported by springs. Although the effective buckling length can be calculated from the beam theory on the elastic floor, it is unsuited for practical design due to its inconvenience.

In addition, the load-bearing capacity curve of the Pier-Pile integral structure supported by the springs at the lower part is different from the application condition of the load-bearing capacity curve shown in the Japan Standard, so its applicability is unclear.

In view of this background, this paper aims to clarify the relationship between the effective buckling length of the Pier-Pile integral structure and characteristic value β specified in the Japanese standards [3; herein after Japan Standard IV]. Furthermore, the load-bearing capacity curve of the pier-pile integral structure with residual stress is to be verified.

In this paper, the aerial part and the underground part of the Pier-Pile integral structure are referred to as "pier" and "pile" respectively.

2 THE EFFECTIVE LENGTH OF THE PIER-PILE INTEGRAL STRUCTURE

2.1 The target structure of the study

The target structure of this study is a single column pier with its lower part supported by spring. Figure 2: A single column pier with lower part supported by spring. It consists of a steel pipe section with an outer diameter of $D=500\text{mm}$, which is the standard size, and a thickness of $9 \leq t \leq 25\text{mm}$, made of SKK490 material as ERW (Electric Resistance Welded) pipes. Young's modulus of the steel is set to $E = 200\text{GPa}$ and Poisson's ratio $\mu=0.3$. The length of a pier is satisfied with the slenderness ratio of $l/r \leq 120$ ($l=Kl_e$, $K=1$ =effective length factor, l_e =length of a pier h , r = cross-section secondary radius); slenderness ratio parameter $\bar{\lambda}$ is calculated with the following formula (1).

$$\bar{\lambda} = 1/\pi \sqrt{\sigma_y/E} l/r \quad (1)$$

Herein, π is the circumference ratio; σ_y is the yield stress of material.

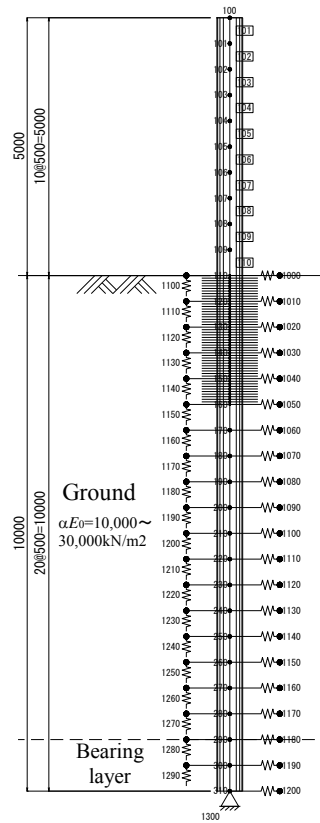


Figure 2: A single column pier with lower part supported by spring.

As it conforms to the Japan Standard IV, the length of pile was set at 10m , based on $\beta L_e > 3$, a semi-infinite-length pile. The ground rigidity is $10\text{MN/m}^2 \leq \alpha E_0 \leq 300\text{MN/m}^2$. The test cases are shown in Table 1 in the form of PP $h(\text{m})$ - $t(\text{mm})$ - αE_0 (MN/m^2). Table 1: *Test cases*.

Table 1: Test cases.

CASE	h (m)/L (m)			diameter and thickness(mm)				ground rigidity αE_0 (MN/mm ²)						
	1/10	5/10	10/10	Φ 500				10	50	100	150	200	250	300
				t=9	t=14	t=19	t=25							
PP1-9-*	○			○				○	○	○	○	○	○	○
PP1-14-*	○				○			○	○	○	○	○	○	○
PP1-19-*	○					○		○	○	○	○	○	○	○
PP1-25-*	○						○	○	○	○	○	○	○	○
PP5-9-*		○		○				○	○	○	○	○	○	○
PP5R-9-*		○		○				○	○	○	○	○	○	○
PP5-14-*		○			○			○	○	○	○	○	○	○
PP5-19-*		○				○		○	○	○	○	○	○	○
PP5-25-*		○					○	○	○	○	○	○	○	○
PP10-9-*			○	○				○	○	○	○	○	○	○
PP10-14-*			○		○			○	○	○	○	○	○	○
PP10-19-*			○			○		○	○	○	○	○	○	○
PP10-25-*			○				○	○	○	○	○	○	○	○

2.2 Analysis model and method

The analysis model is shown in Figure 2.

A hinged end is adopted as the boundary conditions of a pile tip. The pile part is installed with ground springs in horizontal and vertical directions. The ground spring is calculated by the formula based on the Japan Standard IV.

$$k_H = k_{H0} \left(B_H / 0.3 \right)^{-3/4} \quad (2)$$

$$k_{H0} = 1 / 0.3 \alpha E_0 \quad (3)$$

$$B_H = \sqrt{D / \beta} \quad (4)$$

$$\beta = \sqrt[4]{k_H D / 4EI} \quad (5)$$

Herein k_H =horizontal subgrade reaction coefficient, k_{H0} =horizontal subgrade reaction coefficient corresponding to the value of the plate loading test, and $B_H=A$ is the conversion loading width of the foundation. Effective buckling length l_{cr} is determined from the eigenvalue analysis. In the analysis, an axial force of $N = 1$ kN is added to the head of the pier. Then, the primary eigenvalue ω is obtained by calculating the following formula.

$$l_{cr} = \pi \sqrt{EI / \omega N} \quad (6)$$

Herein EI = the flexural rigidity of the steel pipe.

2.3 The relationship between the characteristic value BETA and the effective buckling length of the pile

The effect that the rigidity difference between the ground and the pile has on the effective buckling length l_{cr} is shown in Figure 3. Figure 3: Relationship between the effective buckling length and βh . The vertical axis shows the dimensionless value resulting from dividing the

effective buckling length l_{cr} by the effective buckling length $l_{cr}' = 2h$ when the lower end is fixed. The horizontal axis shows the non-dimensional value resulting from multiplying a pier length h and the characteristic value β of the ground.

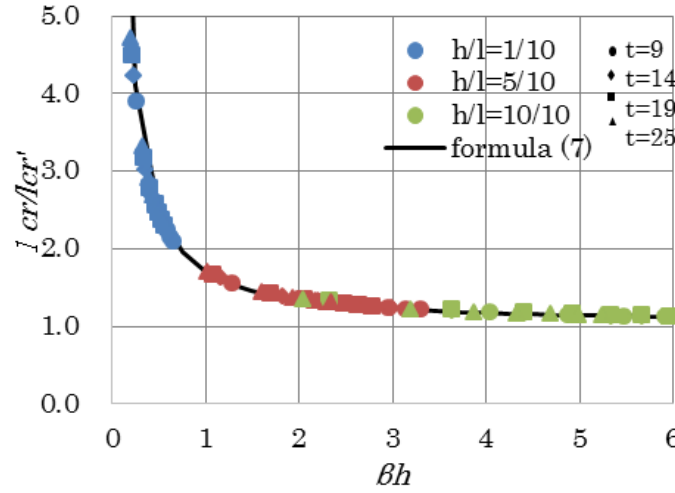


Figure 3: Relationship between the effective buckling length and βh .

From Figure 3, it can be confirmed that as βh increases, namely due to the increase in rigidity of the soil, effective buckling length can be confirmed to approach l_{cr}' . In addition, the relationship of effective buckling length l_{cr} and βh is represented as a continuous curve independent of the pier length and thickness. From the above, the effective buckling length l_{cr} of pier-pile Integral structures is confirmed to be represented by the function of βh .

The authors have indicated that the buckling mode of the pier is convex in the vicinity of the point of M_{\max} and that effective buckling length of the Pier-Pile steel structure is indicated by equation (7), which is twice the length of the Chang equation, $l_m [3] + h.[4]$

$$l_{cr} = 2\alpha_1 \left[h + \frac{1}{\beta} \tan^{-1} \left\{ \frac{1}{(1 + 2\alpha_2 \beta h)} \right\} \right] \quad (7)$$

The variation confirmed in Figure 3 is assumed to be due to the accuracy of analysis α_1 , and the correlation factor α_2 between the dimensionless quantity βh that affect the deformation mode. Herein when the factors are given as $\alpha_1=1.05$ and $\alpha_2=0.1$, the estimated line of (7) is consistent with the analytical value of Figure 3. It should be noted that the correlation function is 0.999, and the standard deviation is 0.042.

3 COMPRESSION CAPACITY OF PIER-PILE INTEGRAL STRUCTURES

3.1 Analysis model and method

Using an analysis model, the Pier-Pile integral structures are studied to research the load-bearing capacity through axial compression analysis. Since this time the subject of study is the buckling of the entire structure, the results from the beam element model used previously in this study were utilized. Compression analysis was conducted for all test cases shown in Table 1.

It is confirmed that the mechanical properties of ERW (Electric Resistance Welded) pipes are higher in yield ratio than the SM material, and the secondary gradient after yield is small [5]. This study focuses on the rigidity relationship between the ground and the piles and the entire buckling phenomenon in the elastic reason when the effective buckling length

increases. Therefore, the mechanical property of this material is as shown in Figure 4; the yield stress is set to 315N/mm^2 , and secondary gradient is level.

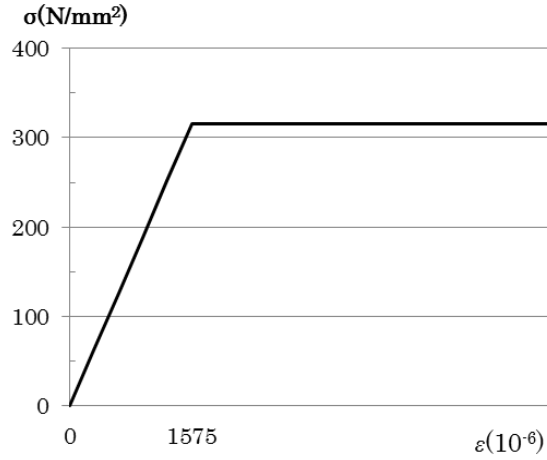


Figure 4: Stress strain curve.

3.2 Distribution of residual stress

The residual stress of ERW pipes is mainly installed in the working process in order to adjust the shape of the product and during the plastic working in the manufacturing process of the pipe. Since the welding heat input of the ERW pipe is extremely small, there is no large tensile residual stress occurring at the welding position. Therefore, residual stress is introduced based on the Aoki method [5] which evaluated residual stress distribution in ERW pipes. Aoki's team evaluated the equivalent axial residual stress σ_{req} derived from the residual stress acting in the circumferential direction and the axial direction respectively, from the residual strain of the ERW pipe measured by the experiment. Equivalent residual stress σ_{req} is defined by equation (8), and the experimental results are measured inside and outside of the ERW pipe, so that the equivalent residual stress is defined in two cases as inside and outside.

$$\sigma_{req} = \bar{\sigma}_x - \left(0.5\bar{\sigma}_\varphi \pm \sqrt{1.0 - 0.75\bar{\sigma}_\varphi^2 - 1.0} \right) \quad (8)$$

The residual stress σ_{req} is shown in Figure 5 as the average value of the inside and outside. The horizontal axis is indicated as the distribution in the circumferential direction, the vertical axis is indicated as the dimensionless value obtained by dividing the residual stress by the yield stress. It is confirmed that the residual stress is distributed on the compression side by an average of about 5% on the yield stress. To briefly express the equivalent residual stress distribution (σ_{req}), assume that the residual stress is given at 36 points on the circumference and the i -th value of is σ_{ri} and the amplitudes are $A_n, B_n, x_i = 1/36, 2/36, \dots, 36/36$; it is defined in accordance with equation (9).

$$\sigma_{ri} = \sum_{j=1}^n A_n \cos 2n\pi x_i + \sum_{j=1}^n B_n \sin 2n\pi x_i \quad (9)$$

In equation (9), coefficients are found by the least squares Fourier decomposition, and when coefficients are obtained using $n = 4, 8, 16$, σ_{ri} is as shown in Figure 9. The solid line shows $n=4$, the dot-dash line is representative of $n=8$, and the double-dots and dash line shows $n=16$. It should be noted that the correlation function is 0.95 ($n=4$), 0.97 ($n=8$), 0.99 ($n=16$). In this study, the equivalent residual stress obtained when $n=4$ is introduced, and two cases, with and without residual stress, are conducted.

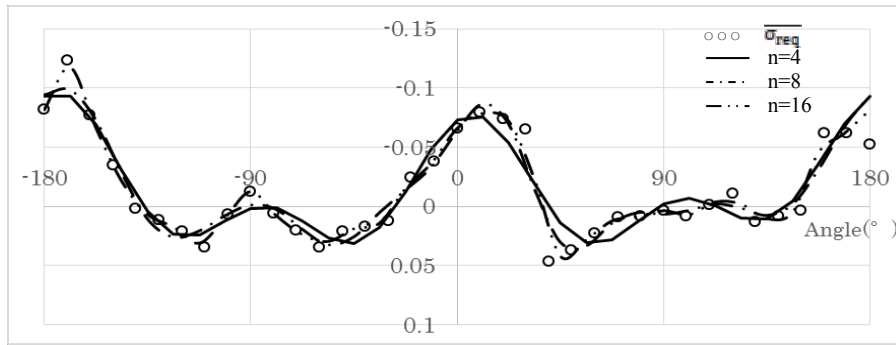


Figure 5: Residual stress distribution of ERW pipe

3.3 The initial deformation

The initial deflection of the Pier-Pile integral structure could be considered as that in the product phase or in the construction phase. In this paper, the aim is to investigate the influence of ground rigidity on the load carrying capacity of the pier-pile integral structure. Therefore, a horizontal displacement of $(h+1)/1000$ is given to the head of pier, and an initial deformation is given so that it becomes the deformation of the primary mode which is provided by eigenvalue analysis. The primary mode is shown in Figure 6.

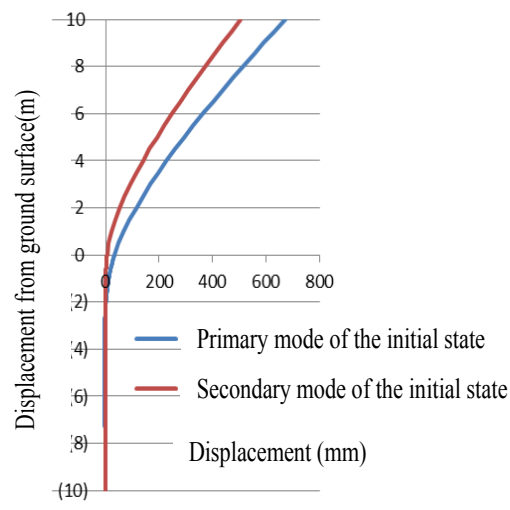
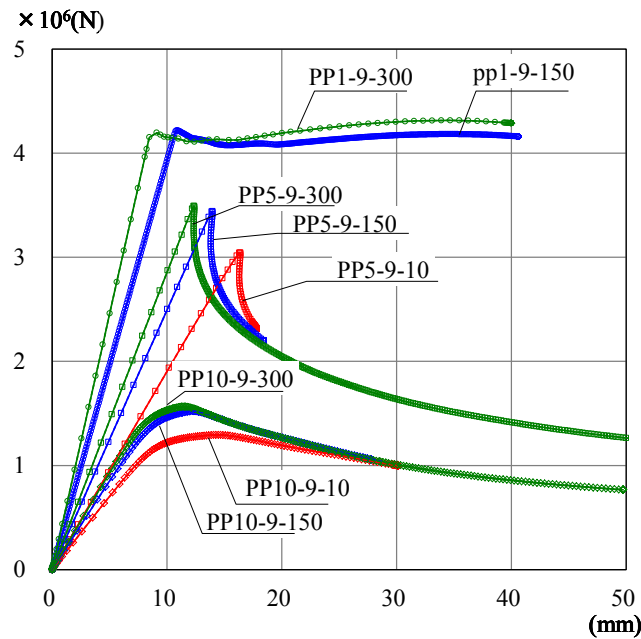


Figure 6: The primary mode of the pier-pile integral structure.

3.4 P - δ curve

The analysis result is shown in Figure 7 as the P - δ curve of the pier top.

It is confirmed from Figure 7 that as the length of the pier increases, the load carrying capacity decreases. In cases where the pier length is the same, it could be seen that the peak value also decreases as the rigidity of the ground decreases. It should be noted that there is almost no difference in load carrying capacity regardless of the presence or absence of residual stress.

Figure 7: P - δ curve.

3.5 Load-bearing capacity curve

The load-bearing capacity curve is shown in Figure 8. The vertical axis represents σ_{cr} / σ_y , that is the dimensionless value generated by dividing generated stress σ_{cr} by σ_y , the yield stress of material which divides the peak of P shown in Figure 7 by a cross-sectional area. And the horizontal axis represents the slenderness ratio parameter. The graph shows the Euler curve; the load-bearing capacity curve of non-prescribed welded box-shaped cross-section from the Japan standard [2], here named curve (a); and the load-bearing capacity curve of the welded box-shaped cross-section, here named curve (b).

The buckling load force curve in each case has a larger load bearing capacity than curve (a) and (b). It should be noted that there is almost no difference due to the the presence or absence of residual stress.

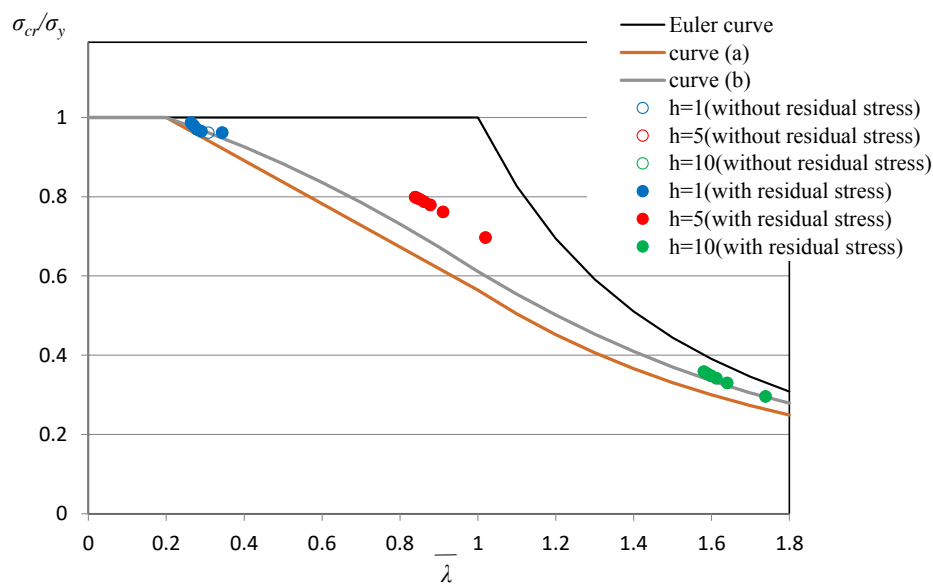


Figure 8: Load-bearing capacity curve.

4 CONCLUSIONS

The following items were revealed in this study.

- Effective buckling length l_{cr} of Pier-Pile integral steel structures can be defined by the simple formula βh .
- The influence of the residual stress on load-bearing capacity of Pier-Pile integral structures is extremely small.
- The load-bearing capacity of Pier-Pile integral structures is slightly larger than the one of Japan Standard II even if including residual stress.

REFERENCES

- [1] schlaich bergermann partner: Award for the footbridge to Le Mont Saint-Michel in France, 2016.2. (<http://www.sbp.de/en/news/award-for-the-footbridge-to-le-mont-saint-michel-in-france-1/>).
- [2] SPECIFICATIONS FOR HIGHWAY BRIDGES PART2 STEEL BRIDGES, Japan Road Association, 2014.
- [3] SPECIFICATIONS FOR HIGHWAY BRIDGES PART4 SUBSTRUCTURES, Japan Road Association, 2014.
- [4] Takayuki Omori, Akira Kasai, Rei Kohara(2016): Numerical Study on Seismic Performance of Pier – Pile Integral Steel Structures with Pipe Section, The 11th Pacific Structural Steel Conference, pp.1149-1154.
- [5] Tetsuhiko AOKI, Yuhshi Fukumoto: STOCHASTIC MATERIAL PROPERTIES AND ESTIMATE OF RESIDUAL STRESSES OF COLD-FORMED-WELDED STEEL TUBULAR MEMBERS WITH SMALL DIAMETER, Proceedings of JSCE, No. 314, pp. 39-51, Oct., 1981.